Evaluation of a Method for Quantification of Restitution Dispersion from the surface ECG

A Mincholé[1,2], E Pueyo[2,1], J.F. Rodríguez[3], E. Zacur[2], M. Doblaré[3,1] and P Laguna[2,1]

[1]Ciber-BBN, Zaragoza, Spain
[2]Comm Techn Group (GTC), Aragon Institute of Eng Research (I3A), University of Zaragoza, Spain
[3]Structural Mechanics and Material Modeling Group (GEMM) at I3A, University of Zaragoza, Spain

Abstract

Spatial dispersion of action potential duration (APD) restitution (APDR) due to electrophysiological heterogeneities in the heart, has been suggested to act as a potent arrhythmogenic substrate. In this work, we evaluate a method aimed at quantifying APDR slope dispersion ($\Delta\alpha$) from the surface electrocardiogram (ECG). A 2D human ventricular in silico tissue preparation is used, from which APDR slope dispersion ($\Delta\alpha^{\text{SIM}}$) at tissue level is computed, and compared with simulated estimates calculated from pseudo-ECGs ($\widehat{\Delta\alpha}^{\text{pECG}}$). We show that $\widehat{\Delta\alpha}^{\text{pECG}}$ values in our simulations are in all cases within the range of clinical values measured from tilt-test recordings. Then, we use the validated tissue model to relate the $\widehat{\Delta\alpha}^{\text{pECG}}$ estimate to measurements of $\Delta\alpha^{\text{SIM}}$, and we prove that the mean error is below 5%. We conclude that the proposed $\widehat{\Delta\alpha}^{\text{pECG}}$ index provides valuable estimates of APDR dispersion with the advantage of being able to be measured non-invasively from the ECG.

1. Introduction

Heart rate (HR) dependence of action potential duration (APD) is thought to be critical in activation instability and, therefore, provides relevant information for ventricular arrhythmic risk stratification [1]. The dynamic APD restitution ($APDR$) curve, measured using the so-called dynamic restitution protocol, quantifies the relationship between the APD and the RR interval (inverse of HR) at steady-state when pacing at different RR intervals [2]. Heterogeneities in the ventricle lead to non uniform restitution properties, which makes $APDR$ curves present spatial variations [3]. Recent studies have suggested that dispersion in the $APDR$ curves may act as a potent arrhythmogenic substrate [4], and increments in that dispersion have been associated with greater propensity to suffer from ventricular tachycardia/fibrillation.

In a previous study [5], a method for quantifying restitution dispersion from the surface electrocardiogram (ECG) was proposed. The proposed ECG measure accounts for the change in the T wave peak to T wave end interval (T_{pe}) at two different stationary RR levels normalized by the difference of the corresponding RR intervals.

In this study, the capability of the proposed ECG measure to provide estimates of $APDR$ slope dispersion at tissue level is assessed by simulating electrical propagation in a 2D tissue preparation representing a slice across the human left ventricular wall, and computing pseudo-ECGs. An electrophysiologically detailed human ventricular cell model [6] is used to generate action potentials. Pacing at different RR intervals is simulated to compute dynamic $APDR$ curves, and eventually $APDR$ slope dispersion. The 2D tissue ventricular model is indirectly validated by comparing the proposed ECG measure evaluated in the simulated pseudo-ECGs with measurements obtained from clinical ECG recordings. Using the validated tissue model, we show that the proposed ECG measure properly quantifies $APDR$ dispersion at tissue level.

2. Methods

2.1. Quantification of Restitution Dispersion from the ECG

Restitution dispersion is quantified from the ECG using the T_{pe} interval, which reflects differences in the time for completion of repolarization by different cells spanning the ventricular wall. Therefore, the T_{pe} interval can be expressed in terms of APDs as follows:

$$T_{pe} = APD_{last} - APD_{min} - \Delta AT \qquad (1)$$

where APD_{min} corresponds to the cell with the minimum APD among those which are currently repolarizing at the T wave peak instant, APD_{last} is the APD of the last cell to repolarize and ΔAT represents the activation time delay between both cells. This ΔAT delay hardly changes with RR for RR intervals above 600 ms [6]. Therefore, deriving T_{pe} with respect to RR, and restricting to the dynamic

protocol, where each value of the $APDR$ curve represents a steady-state APD value:

$$\frac{\partial T_{pe}^{dyn}}{\partial RR} = \frac{\partial APD_{last}^{dyn}}{\partial RR} - \frac{\partial APD_{min}^{dyn}}{\partial RR} \quad (2)$$

where APD^{dyn} and T_{pe}^{dyn} refer to the steady values of APD and T_{pe} for each RR interval. If we let α_{last} and α_{min} denote the slopes of the dynamic restitution curves at the regions corresponding to APD_{last} and APD_{min}, the difference $\Delta\alpha = \alpha_{last} - \alpha_{min}$, which measures dispersion of restitution slopes, can be estimated from the ECG by:

$$\widehat{\Delta\alpha}^{\text{ECG}} = \frac{\Delta T_{pe}^{dyn}}{\Delta RR} \quad (3)$$

where quantification is done by using stable ECG segments, as required in the dynamic protocol, at two different RR intervals.

2.2. Computational modeling and simulation

Computational modeling and simulation is used in this study to assess how the proposed estimate evaluated from the pseudo-ECG, $\widehat{\Delta\alpha}^{\text{pECG}}$, represents dispersion of the $APDR$ slopes at tissue level.

Propagation in a 2D tissue slice 7.5 cm long by 1 cm wide, representing the base to apex and the endocardial to epicardial distances, respectively, as shown in Fig. 1 is simulated using the human ten Tusscher action potential model [6], with numerical integration performed as described in [7]. The ten Tusscher model describes the principal ionic currents through the cardiac cell membrane with high degree of electrophysiological detail for the three types of cells in the ventricular wall: endo-, mid- and epicardial cells. The conductivity of the tissue along the fiber direction is set to σ_L= 0.0013 cm^2/ms, which leads to a maximum conduction velocity of 71 cm/s. Perpendicular to the fiber direction, the conductivity is σ_T= 0.00052 cm^2/ms, resulting in a conduction velocity of 42 cm/s, based on [8]. A transmural linear variation of the helix fiber angle from +60 degrees at the endocardium to -60 degrees at the epicardium is assumed based on [9].

As illustrated in Fig. 1, two areas are stimulated simultaneously: 1 cm at the top of the base and 0.5 cm at the bottom of the apex, based on the activation sequence reported for an isolated human heart in [10]. Transmural heterogeneities are included in the 2D tissue preparation by using two cell types: midmyocardial and epicardial cells. In order to match the complete activation sequence of [10] and to account for the influence of Purkinje fibers, endocardial cells in the simulated preparation are replaced with midmyocardial cells, known to have longer APDs.

The distribution of cell types in the simulated tissue is 80% of midmyocardial cells and 20% of epicardial cells

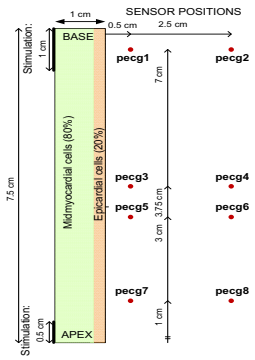

Figure 1. 2D tissue slice used in the simulation, with indication of the default cell type distribution across the ventricular wall, and sensor positions used for pseudo-ECG computation.

[11]. To represent possible heterogeneities in human hearts and measure a range of plausible restitution dispersion values, the effect of varying the percentages of cell types within the ventricular wall is evaluated by considering additional distributions of 65/35% and 90/10% of midmyocardial/epicardial cells. For each cell type distribution, $APDR$ curves are computed by pacing the 2D tissue preparation at different RR intervals, following the so-called dynamic restitution protocol [12]. Dispersion of $APDR$ slopes at tissue level is denoted by $\Delta\alpha^{\text{SIM}}$ and is computed from the results of the 2D simulation as follows:

$$\Delta\alpha^{\text{SIM}} = \frac{\partial APD_{last}^{dyn}}{\partial RR} - \frac{\partial APD_{min}^{dyn}}{\partial RR} \quad (4)$$

where APD_{min}^{dyn} and APD_{last}^{dyn} are defined as described in section §2.1. Estimations of $\Delta\alpha^{\text{SIM}}$ are computed from each pseudo-ECG (each one measuring the extracellular potential at one of the sensor positions shown in Fig. 1):

$$\widehat{\Delta\alpha}^{\text{pECG}} = \frac{\partial T_{pe}^{dyn}}{\partial RR} \quad (5)$$

3. Results

3.1. Evaluation of the 2D simulations: Comparison between pseudo-ECGs and clinical ECGs

The 2D tissue model preparation yields an activation sequence that is in good agreement with the experimental results reported in [10]. Fig. 2 shows a simulated sequence of voltage representation during steady-state pacing at 1000 ms, with indication of the timing corresponding to the T wave peak and T wave end in the pseudo-ECG, and of the regions where APD_{min} and APD_{last} are computed. Since our 2D preparation includes only transmural heterogeneities, the time instant corresponding to the peak

of the T wave coincides with the time at which complete repolarization of the epicardium occurs.

In Fig.3, the difference between APD_{last}^{dyn} and APD_{min}^{dyn} is compared with the steady-state T_{pe}^{dyn} interval computed at different sensor positions (**pecg1** and **pecg5**). Note that ΔAT (not shown in Fig. 3) is constant during the whole RR range.

As an indirect validation of our 2D tissue model, steady-state T_{pe}^{dyn} values computed at different RR intervals in tilt test ECGs and in simulated pseudo-ECGs are compared. Fig. 4 shows three regions corresponding to simulations using cell type distributions of 65/35%, 80/20% and 90/10%. Each region represents the range of steady-state [RR, T_{pe}^{dyn}] curves computed for pseudo-ECGs at eight different sensor positions. The upper curve corresponds to **pecg1** and the lower to **pecg5** sensor positions. The steady-state [RR, T_{pe}^{dyn}] values obtained from the tilt test recordings are superimposed in the same graphic. Simulated values of T_{pe} at different RR intervals for 65/35% and 80/20% (default) cell type distributions are found to be within the range of values measured from the tilt test recordings. However, simulated T_{pe} values for the 90/10% percentage are outside the range of the tilt test recordings.

After confirming the good agreement of the [RR, T_{pe}^{dyn}] curves between pseudo-ECGs and clinical ECGs, the restitution dispersion estimates are also compared. Table 1 quantifies the differences between pseudo-ECG-based estimates of $APDR$ dispersion, $\widehat{\Delta\alpha}^{\text{pECG}}$ (equation (5)), at sensor positions **pecg1** and **pecg5**, and ECG-based estimates, $\widehat{\Delta\alpha}^{\text{ECG}}$ (equation (3)), obtained from the tilt test recordings described in [5]. Both the average difference between $\widehat{\Delta\alpha}^{\text{pECG}}$ (computed in **pecg1** and **pecg5**) and $\widehat{\Delta\alpha}^{\text{ECG}}$, and the average percentage of the difference are shown in Table 1. Differences are below 20% in mean, which are within physiological variability limits.

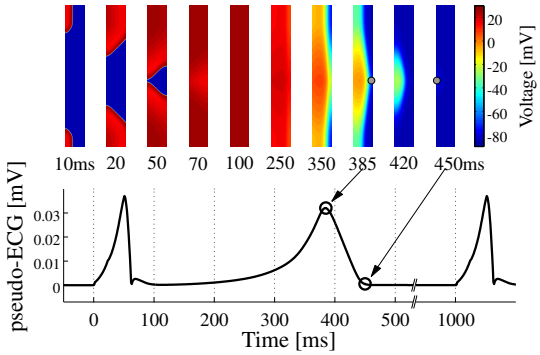

Figure 2. Top panel: simulated sequence of isochronic voltage representation during steady-state pacing at 1000 ms. The position of the two cells corresponding to APD_{min} for the peak of the T wave and APD_{last} for the end of the T wave, are shown with a gray point. Bottom panel: derived pseudo-ECG.

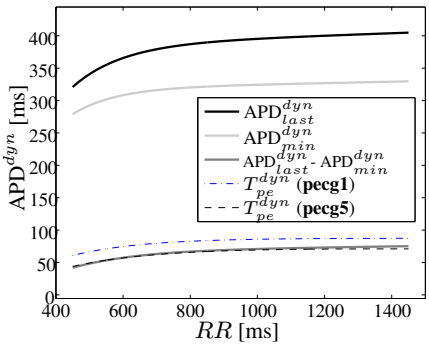

Figure 3. For 80/20% cell type distribution, $APDR$ curves and their relation with steady-state T_{pe}^{dyn} interval derived from **pecg1** and **pecg5** are shown.

Simulated - Measured	*Cell Percent.*	Average (%)
$\widehat{\Delta\alpha}^{\text{pECG}}$ (**pecg1**) - $\widehat{\Delta\alpha}^{\text{ECG}}$	(65/35%)	-0.0096 (-19%)
	(80/20%)	-0.0107 (-23%)
$\widehat{\Delta\alpha}^{\text{pECG}}$ (**pecg5**) - $\widehat{\Delta\alpha}^{\text{ECG}}$	(65/35%)	-0.0089 (-16%)
	(80/20%)	-0.0084 (-10%)

Table 1. Average value across subjects of the difference between the estimates measured from the simulated pseudo-ECGs in **pecg1** and **pecg5** ($\widehat{\Delta\alpha}^{\text{pECG}}$), and from the tilt test recordings $\widehat{\Delta\alpha}^{\text{ECG}}$. Different percentages of cell types have been used to derive the pseudo-ECGs.

3.2. Assessment of $APDR$ dispersion quantified from the pseudo-ECG

$APDR$ slope dispersion at tissue level, denoted by $\Delta\alpha^{\text{SIM}}$ (equation (4)), has been computed for each of the three cell type distributions. $\Delta\alpha^{\text{SIM}}$ is used to assess whether $\widehat{\Delta\alpha}^{\text{pECG}}$, computed from pseudo-ECGs, is a good estimate of $APDR$ slope dispersion. Fig. 5 shows the comparison between $\Delta\alpha^{\text{SIM}}$ and $\widehat{\Delta\alpha}^{\text{pECG}}$ computed at sensor positions **pecg3** and **pecg5** for the default cell type distribution 80/20%. The error between $\Delta\alpha^{\text{SIM}}$ and $\widehat{\Delta\alpha}^{\text{pECG}}$ from

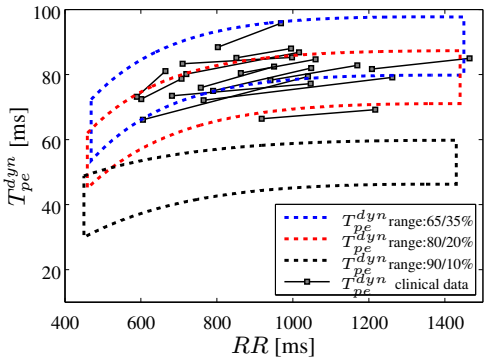

Figure 4. T_{pe}^{dyn} as a function of RR from tilt test recordings (in squares) and from simulations. For the simulations, the regions correspond to cell type distributions of 65/35%, 80/20% and 90/10%, and each region represents the influence of computing steady-state [RR, T_{pe}^{dyn}] curves for pseudo-ECGs at different sensor positions.

both **pecg1** and **pecg5**, relative to the slope range, is found to be 5% in average.

4. Discussion and Conclusions

In this study, electrical propagation in a cardiac tissue has been simulated to assess the validity of a method aimed at quantifying APD restitution dispersion from the surface ECG. The characteristics of the tissue and cell model have been shown to be adequate for the purpose of the study. On one hand, the ten Tusscher cell model considered in this study has been shown to reproduce experimentally observed data on APD restitution in single cells from epi, endo and midmyocardial regions correctly [6]. Characteristics of the 2D tissue model proposed in this work, such as dimensions, conduction velocities [6, 8], transmural variation of the fiber angle [9], and heterogeneity of cell types across the ventricular wall [11], are in agreement with experimental studies. The simulated activation sequences is in good agreement with those obtained in isolated human heart sections reported in [10].

Experimental studies in canine wedge preparations [8] show that in case of having transmural heterogeneities only, the time instant of the T wave peak corresponds to the complete repolarization of the epicardium. This agrees with results from our 2D simulations, which include only transmural heterogeneities, where the peak of the T wave in pseudo-ECGs coincides with the total repolarization of the epicardium in the central part of the tissue (see the isochronic voltage representation in Fig. 2).

We have also evaluated repolarization and restitution properties by showing that T_{pe}^{dyn} values and the estimates $\widehat{\Delta\alpha}^{\text{pECG}}$, derived from the pseudo-ECGs, are within the range measured in clinical tilt test recordings.

After validating the 2D tissue preparation, $\widehat{\Delta\alpha}^{\text{pECG}}$, measured from the pseudo-ECG, has been shown to properly quantify $APDR$ slope dispersion $\Delta\alpha^{\text{SIM}}$ at tissue level, being the mean error relative to the slope range below 5% (see Fig. 5).

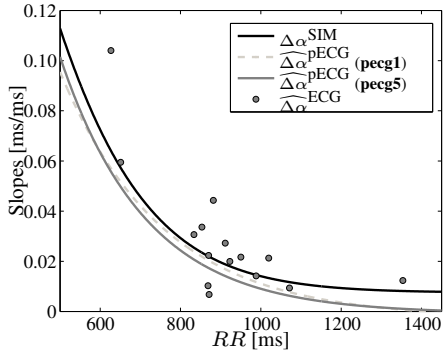

Figure 5. APDR slope dispersion, $\Delta\alpha^{\text{SIM}}$, for the cell type distribution 80/20%, the proposed estimate measured from the pseudo-ECG in **pecg1** and **pecg5**, and the estimates measured from the tilt test recordings.

In brief, the ECG estimate proposed in this study provides a valuable quantification of $APDR$ dispersion, being able to be measured non-invasively from the surface ECG.

Acknowledgements

This work was financially supported by grants TEC2007- 68076-C02-02/TCM from MCyT and FEDER, Spain, PI 165/09 from CONAI+D, DGA, Spain, and PI144/2009 from Gobierno de Aragon, Spain.

References

[1] Rosenbaum DS, Jackson LE, Smith JM, Garan H, Ruskin JN, J. CR. Electrical alternans and vulnerability to ventricular arrhythmias. N Engl J Med 1994;330(4):235–241.

[2] Franz MR, Swerdlow CD, Liem LB, Schaefer J. Cycle Length Dependence of Human Action Potential Duration In Vivo. J Clin Invest 1988;82:972–979.

[3] Laurita KR, Girouard SD, Rosenbaum DS. Modulation of ventricular repolarization by a premature stimulus: Role of epicardial dispersion of repolarization kinetics demonstrated by optical mapping of the intact guinea pig heart. Circ Res 1996;79:493–503.

[4] Nash M, Bradley C, Sutton P, Clayton R, Kallis P, Hayward M, Paterson D, Taggart P. Whole heart action potential duration restitution properties in cardiac patients: a combined clinical and modelling study. Experimental physiology 2006;91(2):339–54.

[5] Mincholé A, Pueyo E, Laguna P. Transmural differences in rate adaptation of repolarization duration quantified from ECG repolarization interval dynamics. In XXXVI Ann. Conf. Computers in Cardiology. 2009; 597–600.

[6] Ten Tusscher K, Panfilov A. Alternans and spiral breakup in a human ventricular tissue model. Am J Physiol Heart Circ Physiol 2006;291(3):H1088–H1100.

[7] Heidenreich E, Ferrero JM, Doblaré M, Rodríguez JF. Adaptive macro finite elements for the numerical solution of monodomain equations in cardiac electrophysiology. Annals of Biomedical Engineering 2010;38:2331–2345.

[8] Yan GX, Shimizu W, Antzelevitch C. Characteristics and distribution of M cells in arterially perfused canine left ventricular wedge preparations. Circ 1998;98:1921–1927.

[9] Streeter DD, Spotnitz HM, Patel DP, Ross J, Sonnenblick EH. Fiber Orientation in the Canine Left Ventricle during Diastole and Systole. Circ Res 1969;24:339–347.

[10] Durrer D, van Dam RT, Freud GE, Janse MJ, Meijler FL, Arzbaecher RC. Total Excitation of the Isolated Human Heart. Circulation 1970;41:899–912.

[11] Drouin E, Charpentier F, Gauthier C, Laurent K, Le-Marec H. Electrophysiologic characteristics of cells spanning the left ventricular wall of human heart: Evidence for presence of M cells. Am J Physiol Heart Circ Physiol 1995; 26(1):185–192.

[12] Riccio ML, Koller ML, Gilmour Jr RF. Electrical Restitution and Spatiotemporal Organization During Ventricular Fibrillation. Circ Res 1999;84:955–963.